IRAQI STATISTICIANS JOURNAL

https://isj.edu.iq/index.php/isj

ISSN: 3007-1658 (Online)

The Odd Exponential–Rayleigh-Fréchet Distribution: Structural Properties, Estimation Methods, and Applications

Raghad W. Faris[1], Mundher A. khaleel [2]

[1,2] Mathematics Departments, College of Computer Science and Mathematics, Tikrit University, 34001 Baghdad, Iraq.

ARTICLE INFO

Article history:
Received 27 November 2025
Revised 27 November 2025
Accepted 13 January 2026
Available online 16 January 2026

Keywords:
Exponential–Rayleigh-Fréchet
Odd Exponential–Rayleigh-G
survival function
QLS
MLE

ABSTRACT

This research presents a novel probability model called the Odd Exponential–Rayleigh–Fréchet (OERFR) distribution, which combines the power of the Odd-Exponentiated Rayleigh probability transformation with the flexibility of the Fréchet distribution, known for its ability to represent data with heavy tails and extreme values. The new model aims to address the problems that arise when using traditional distributions in the analysis of reliability and engineering data characterized by significant skewness and nonlinearity in risk behavior. The mathematical construction of the distribution is based on combining the T-X transformation with the odd-ratio transformation, adding two additional shape parameters to the basic distribution. These parameters enhance the distribution's ability to control tail shape, density slope, and the variety of risk function shapes. The basic functions of the model were derived. The study included conducting extensive simulation experiments using eight different estimation methods and at various sample sizes to evaluate the accuracy and statistical stability of each method. The results showed that some methods, such as QLS, MP, and WLSE, were superior in reducing bias and root-squared error at small and medium sample sizes. To confirm the applicability of the distribution, the model was tested on real data representing turbocharger failure times for diesel trucks. The OERFR model demonstrated a clear advantage over several competing distributions according to AIC, BIC, KS, AD, and CV metrics. This performance indicates that the new distribution possesses high flexibility and strong ability to represent real-world data in the areas of engineering, reliability, and extreme value analysis.

1. Introduction

Extended-elasticity parametric probability distributions are a focus of contemporary statistical literature and play a crucial role in modeling reliability and survival data, as well as in extrema analysis and the interpretation of complex phenomena in engineering and applied sciences. While traditional models, such as the classical Rayleigh and Whipple distributions, retain their importance due to their ease of interpretation, their structural limitations often prevent them from accommodating the complex statistical properties of real-world data, particularly data characterized by high skewness, thick tails, and, most importantly, non-unmodal hazard shape behavior.

To bridge this methodological gap, theoretical and applied statistics have witnessed a surge in the development of generalized distribution families that extend the basic models by integrating them with innovative probability generators. The T-X transformer approach, developed by Alzaatreh and colleagues (2013) [1], is a pioneering model and one of the most prominent methodological

Corresponding Author: rwamedh@tu.edu.iq
https://doi.org/10.62933/rqcrpb69

frameworks that has enabled researchers to produce distributions capable of adding additional shape parameters to increase modeling flexibility.

This approach has yielded a wide range of robust distribution families that generalize traditional models, most notably: Inverted Topp–Leone-H family [2], Shifted Exponential-G (SHE-G) generator [3], Novel Logarithmic Approach [4], NGLog-X Family [5], Lomax extended exponentiated-X [6], Odd Lomax-G family [7], Generalized Odd Maxwell-Generated [8], hybrid odd exponential [9], Modified type-II family [10] and similar proposals that utilize other transformations.

Building on this innovative path, and in the context of searching for models with extended operand flexibility to model failure data exhibiting extreme values and complex risk patterns, this research presents a family of probability distributions. A new model, called the Odd Exponentiated Rayleigh Fréchet (OERFR) distribution, combines the originality of the mathematical transformation with the strength of the underlying models. OERFR is constructed by incorporating the generative core of the exponential Rayleigh distribution within a T-X framework, in conjunction with the Odd Ratio Transformation, the Odd Exponentiated Rayleigh (OER-G) family has a CDF and pdf with forms, respectively:

$$G_{OER}(x,\delta,\theta,\phi)=\left(1-e^{-\delta\left[\frac{F(x,\phi)}{1-F(x,\phi)}\right]^2}\right)^{\theta} \quad (1)$$

$$g_{OER}(x,\delta,\theta,\phi)=\frac{2\delta\theta f(x,\phi)F(x,\phi)}{[1-F(x,\phi)]^3}e^{-\delta\left[\frac{F(x,\phi)}{1-F(x,\phi)}\right]^2}\left(1-e^{-\delta\left[\frac{F(x,\phi)}{1-F(x,\phi)}\right]^2}\right)^{\theta-1} \quad (2)$$

where δ,θ are shape parameters for a family, and $F(x,\phi)$ is any baseline distribution.

Using the robust Fréchet distribution $F(x,\phi)$as the underlying distribution. The Fréchet distribution is known for its importance in modeling extreme values and thick-tailed phenomena, making it ideal for reliability analysis. This configuration incorporates three additional shape parameters that give OERFR exceptional control over the thickness of the distribution's tail, skewing, and hazard rate dynamics. This proposal underscores the research activity in generalized Odd families, as demonstrated by recent work such as the Odd Lomax-G study by [11] .

2. The Odd Exponential–Rayleigh-Fréchet Distribution

To

Take the Fréchet (FR) distribution as a baseline model, with CDF and PDF respectively are $F(x,\beta,\xi)=e^{-\beta x^{-\xi}}$ and $g(x,\beta,\xi)=\beta\xi x^{-(\xi+1)}e^{-\beta x^{-\xi}}$ [12] and to find Fréchet baseline for OERG by puttying the last equations in Eq.(1), and Eq.(2) to have the CDF and PDF of Odd Exponentiated Rayleigh Fréchet (OERFR) dist. by forms:

$$G_{OERFR}(x,\delta,\theta,\beta,\xi)=\left(1-e^{-\delta\left[\frac{e^{-\beta x^{-\xi}}}{1-e^{-\beta x^{-\xi}}}\right]^2}\right)^{\theta},\ x\geq 0,\ \delta,\theta,\beta,\xi>0 \quad (3)$$

$$g_{OERFR}(x,\delta,\theta,\beta,\xi)=\frac{2\delta\theta\beta\xi x^{-(\xi+1)}e^{-2\beta x^{-\xi}}}{\left[1-e^{-\beta x^{-\xi}}\right]^3}e^{-\delta\left[\frac{e^{-\beta x^{-\xi}}}{1-e^{-\beta x^{-\xi}}}\right]^2}\left(1-e^{-\delta\left[\frac{e^{-\beta x^{-\xi}}}{1-e^{-\beta x^{-\xi}}}\right]^2}\right)^{\theta-1} \quad (4)$$

where δ,θ,β,ξ are shape parameters for OERFR

While the survival function for OERFR can be founded by form [13]:

$$S_{OERFR}(x,\delta,\theta,\beta,\xi)=1-G_{OERFR}(x,\delta,\theta,\beta,\xi)$$

$$S_{OERFR}(x,\delta,\theta,\beta,\xi)=1-\left(1-e^{-\delta\left[\frac{e^{-\beta x^{-\xi}}}{1-e^{-\beta x^{-\xi}}}\right]^2}\right)^{\theta} \quad (5)$$

While the hazard function for OERFR can be founded by form [14]:

$$h_{OERFR}(x,\delta,\theta,\beta,\xi)=\frac{g_{OERFR}(x,\delta,\theta,\beta,\xi)}{S_{OERFR}(x,\delta,\theta,\beta,\xi)}$$

$$h_{OERFR}(x,\delta,\theta,\beta,\xi)=\frac{\dfrac{2\delta\theta\beta\xi x^{-(\xi+1)}e^{-2\beta x^{-\xi}}}{\left[1-e^{-\beta x^{-\xi}}\right]^{3}}e^{-\delta\left[\frac{e^{-\beta x^{-\xi}}}{1-e^{-\beta x^{-\xi}}}\right]^{2}}\left(1-e^{-\delta\left[\frac{e^{-\beta x^{-\xi}}}{1-e^{-\beta x^{-\xi}}}\right]^{2}}\right)^{\theta-1}}{1-\left(1-e^{-\delta\left[\frac{e^{-\beta x^{-\xi}}}{1-e^{-\beta x^{-\xi}}}\right]^{2}}\right)^{\theta}} \quad (6)$$

The figures 1, 2, and 3 shows the CDF, pdf, and survival functions with different values of δ,θ,β,ξ, respictivaly.

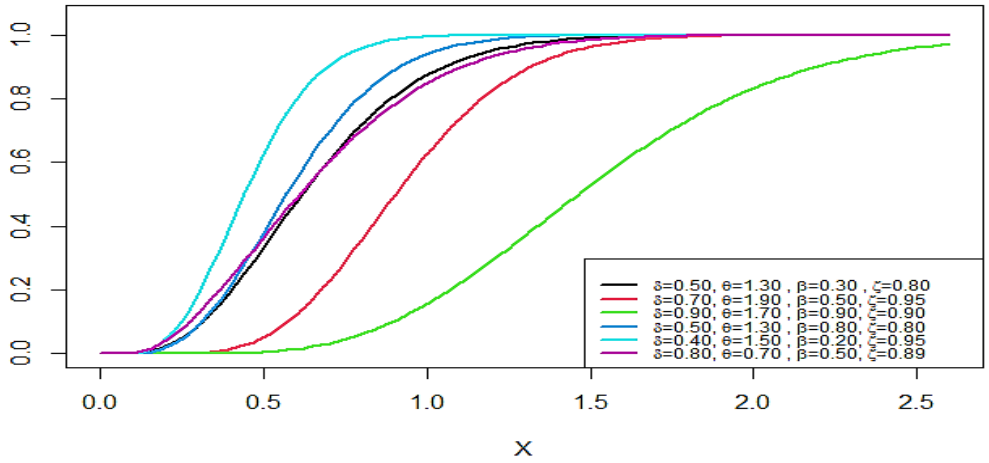

Figure 1. plot CDF function for OERFR with different values of δ,θ,β,ξ

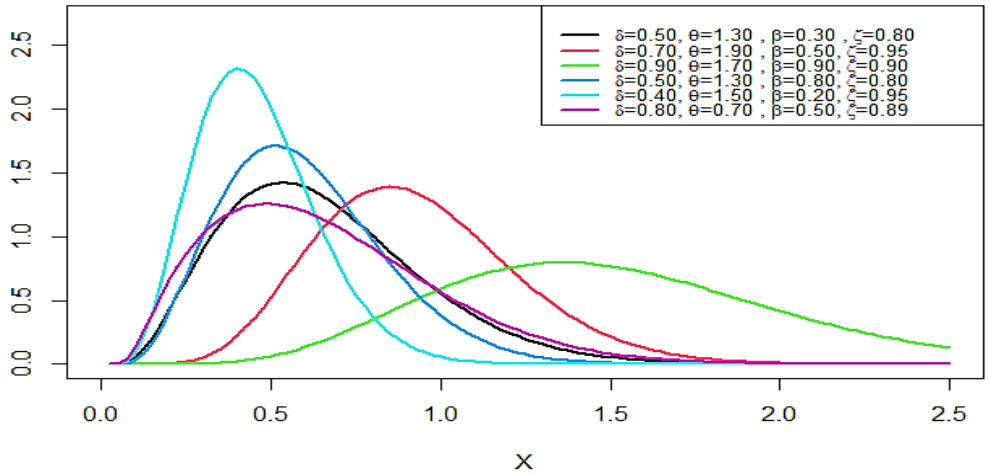

Figure 2. plot pdf function for OERFR with different values of δ,θ,β,ξ

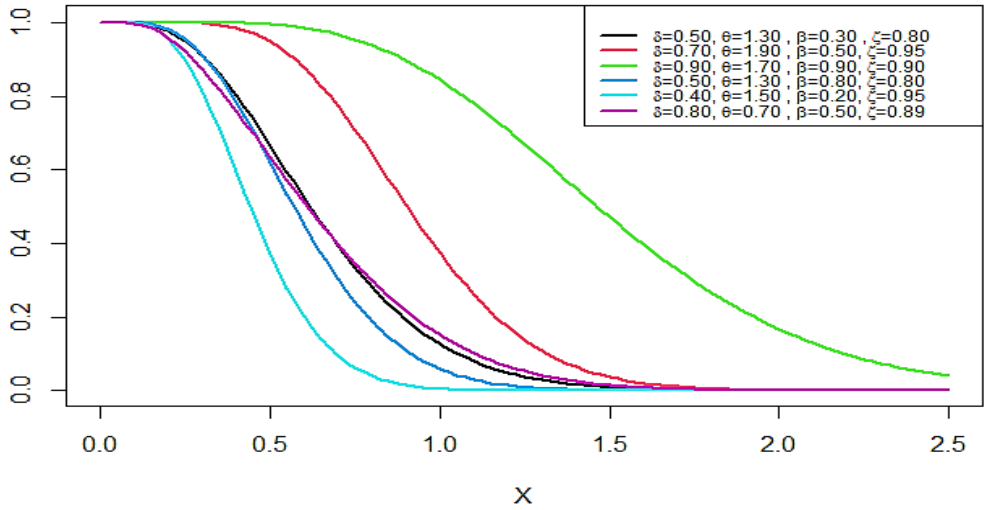

Figure 3. plot survival function for OERFR with different values of $\delta, \theta, \beta, \xi$

Figure 1 illustrates the cumulative behavior of the cumulative distribution function of the OERFR distribution at different parameter values. The graph shows that increasing parameter height shifts the distribution curve to the right and increases its slope, reflecting the increasing probability of large values. The figure also demonstrates the distribution's ability to represent data with heavy tails and significant skewness, as the speed of the distribution's ascent varies with the parameter changes. This indicates the model's flexibility in representing different data patterns.

Figure 2 shows the change in density shape between concentricity and diffusion, as well as the emergence of multiple possible density shapes, from a single-peak curve to a rightward-sloping curve. This behavior reflects the crucial role of parameters in controlling the distribution's shape, particularly in determining the height and position of the peak and the extent of the right tail. This proves the distribution's ability to model data with extreme values.

Figure 3 represents the survival function of the distribution and shows how the probability of survival decreases as the variable values increase. This demonstrates the distribution's ability to accurately represent the failure or collapse behavior of dependency data, as the rate of decrease varies with the parameters. When the tail is heavier, the survival function slows down, indicating a higher probability of large values.

3. Some properties for OERFR

3.1 Expansion CDF and pdf for OERFR

Due to the difficulty in dealing with CDF and pdf functions in deriving some statistical properties of the distribution, these functions are expanded using the binomial expansion and the expansion of the exponential function, as follows: For the CDF function defined in Eq.(3), it is expanded as follows: using binomial expansion to get:

$$\left(1-e^{-\delta\left[\frac{e^{-\beta x^{-\xi}}}{1-e^{-\beta x^{-\xi}}}\right]^2}\right)^{\theta} = \sum_{i=0}^{\infty}(-1)^i\binom{\theta}{i}e^{-\delta\left[\frac{e^{-\beta x^{-\xi}}}{1-e^{-\beta x^{-\xi}}}\right]^{2i}}$$

Using exponential expansion for $e^{-\delta\left[\frac{e^{-\beta x^{-\xi}}}{1-e^{-\beta x^{-\xi}}}\right]^{2i}}$ to get:

$$e^{-\delta\left[\frac{e^{-\beta x^{-\xi}}}{1-e^{-\beta x^{-\xi}}}\right]^{2i}} = \sum_{l=0}^{\infty}\frac{(-1)^{2i+l}}{l!}\delta^l\left(\frac{e^{-\beta x^{-\xi}}}{1-e^{-\beta x^{-\xi}}}\right)^l$$

$$e^{-\delta\left[\frac{e^{-\beta x^{-\xi}}}{1-e^{-\beta x^{-\xi}}}\right]^{2i}}$$

$$=\sum_{l=0}^{\infty}\frac{(-1)^{2i+l}}{l!}\delta^{l}\frac{e^{-l\beta x^{-\xi}}}{\left(1-e^{-\beta x^{-\xi}}\right)^{l}}$$

And using [15]:

$$G_{OERFR}(x,\delta,\theta,\beta,\xi)=\sum_{i=0}^{\infty}\sum_{l=0}^{\infty}\sum_{j=0}^{\infty}\frac{(-1)^{3i+l}\Gamma(l+j)}{j!\,l!\,\Gamma(l)}\binom{\theta}{i}\delta^{l}e^{-\beta(l+j)x^{-\xi}}$$

Or

$$G_{OERFR}(x,\delta,\theta,\beta,\xi)=He^{-\beta(l+j)x^{-\xi}}$$

where

$$H=\sum_{i=0}^{\infty}\sum_{l=0}^{\infty}\sum_{j=0}^{\infty}\frac{(-1)^{3i+l}\Gamma(l+j)}{j!l!\Gamma(a)}\binom{u}{i}\delta^{l}$$

$$G_{OERFR}^{\lambda}(x,\delta,\theta,\beta,\xi)=\left(1-e^{-\delta\left[\frac{e^{-\beta x^{-\xi}}}{1-e^{-\beta x^{-\xi}}}\right]^{2}}\right)^{\lambda\theta}$$

Can be expanded as form:

$$G_{OERFR}^{\lambda}(x,\delta,\theta,\beta,\xi)=Re^{-\beta(z+w)x^{-\xi}}$$

where

$$R=\sum_{v=0}^{\infty}\sum_{z=0}^{\infty}\sum_{w=0}^{\infty}\frac{(-1)^{3v+z}\Gamma(z+w)}{w!z!\Gamma(z)}\binom{\lambda\theta}{v}\delta^{z}$$

while the pdf expansion can be found as follows:

$$\left(1-e^{-\delta\left[\frac{e^{-\beta x^{-\xi}}}{1-e^{-\beta x^{-\xi}}}\right]^{2}}\right)^{\theta-1}$$

$$=\sum_{s=0}^{\infty}(-1)^{s}\binom{\theta-1}{i}e^{-\delta s\left[\frac{e^{-\beta x^{-\xi}}}{1-e^{-\beta x^{-\xi}}}\right]^{2}}$$

$$e^{-\delta(s+1)\left[\frac{e^{-\beta x^{-\xi}}}{1-e^{-\beta x^{-\xi}}}\right]^{2}}$$

$$=\sum_{p=0}^{\infty}\frac{(-1)^{2(s+1)+p}}{p!}\delta^{p}(s+1)^{p}\left(\frac{e^{-\beta x^{-\xi}}}{1-e^{-\beta x^{-\xi}}}\right)^{2p}$$

$$g_{OERE}(x,\delta,\theta,\beta,\xi)=Kx^{-(\xi+1)}e^{-\beta[2(p+1)+q]x^{-\xi}}$$

Where

$$K=\sum_{s=0}^{\infty}\sum_{p=0}^{\infty}\sum_{q=0}^{\infty}\frac{\Gamma(p+3+q)(-1)^{2(s+1)+p+s}}{q!p!\Gamma(p+3)}\binom{\theta-1}{i}2\delta\theta\beta\xi\delta^{p}(s+1)^{p}$$

3.2 Moment function

$$(1-t)^{-a}=\sum_{i=0}^{\infty}\frac{\Gamma(a+i)}{i!\,\Gamma(a)}t^{i}$$

$$\left(1-e^{-\beta x^{-\xi}}\right)^{-l}=\sum_{j=0}^{\infty}\frac{\Gamma(l+j)}{j!\,\Gamma(l)}e^{-j\beta x^{-\xi}}$$

Then the final form for CDF is:

(7)

while the $G_{OERFR}^{\lambda}(x,\delta,\theta,\beta,\xi)$ which has a form:

(8)

(9)

$$g_{OERFR}(x,\delta,\theta,\beta,\xi)$$

$$=\sum_{s=0}^{\infty}\sum_{p=0}^{\infty}\frac{(-1)^{2(s+1)+p+s}}{p!}\binom{\theta-1}{i}\delta^{p}(s+1)^{p}\left(\frac{e^{-\beta x^{-\xi}}}{1-e^{-\beta x^{-\xi}}}\right)^{2p}\frac{2\delta\theta\beta\xi x^{-(\xi+1)}e^{-2\beta x^{-\xi}}}{\left[1-e^{-\beta x^{-\xi}}\right]^{3}}$$

$$g_{OERFR}(x,\delta,\theta,\beta,\xi)$$

$$=\sum_{s=0}^{\infty}\sum_{p=0}^{\infty}\frac{(-1)^{2(s+1)+p+s}}{p!}\binom{\theta-1}{i}2\delta\theta\beta\xi\delta^{p}(s+1)^{p}\frac{x^{-(\xi+1)}e^{-2\beta(p+1)x^{-\xi}}}{\left(1-e^{-\beta x^{-\xi}}\right)^{2p+3}}\left(1-e^{-\beta x^{-\xi}}\right)^{-2p-3}$$

$$=\sum_{q=0}^{\infty}\frac{\Gamma(p+3+q)}{q!\,\Gamma(p+3)}e^{-\beta q x^{-\xi}}$$

Then the final form for pdf is:

(10)

For any random variable X, the moment of order m for OERFR distribution given with Eq. (10) in form:

$$\mu_{m}(x)$$

$$=K\int_{0}^{\infty}x^{m}x^{-(\xi+1)}e^{-\beta[2(p+1)+q]x^{-\xi}}\,dx$$

$$\mu_m(x) = K\int_0^{\infty} x^{m-(\xi+1)} e^{-\beta[2(p+1)+q]x^{-\xi}}\, dx$$

Let $y = \beta[2(p+1)+q]x^{-\xi} \rightarrow x^{-\xi} = \frac{y}{\beta[2(p+1)+q]} \rightarrow x = \sqrt[\xi]{\frac{\beta[2(p+1)+q]}{y}} \rightarrow dx = -\frac{1}{\xi}(\beta[2(p+1)+q])^{\frac{1}{\xi}} y^{-\frac{(\xi+1)}{\xi}} dy$

$$\mu_m(x) = -K\int_0^{\infty} \left(\sqrt[\xi]{\frac{\beta[2(p+1)+q]}{y}}\right)^{m-(\xi+1)} e^{-y}\frac{1}{\xi}(\beta[2(p+1)+q])^{\frac{1}{\xi}} y^{-\frac{(\xi+1)}{\xi}} dy$$

Then the final form for moment function is:

$$\mu_m(x) = \frac{K}{\xi}(\beta[2(p+1)+q])^{\frac{m}{\xi}-1}\Gamma\left(1-\frac{m}{\xi}\right) \quad (11)$$

Then the 1st-4th moment for OERFR distribution given from Eq. (11) in forms:

$$\mu_1 = \frac{K}{\xi}(\beta[2(p+1)+q])^{\frac{1}{\xi}-1}\Gamma\left(1-\frac{1}{\xi}\right) \quad (12)$$

$$\mu_2 = \frac{K}{\xi}(\beta[2(p+1)+q])^{\frac{2}{\xi}-1}\Gamma\left(1-\frac{2}{\xi}\right) \quad (13)$$

$$\mu_3 = \frac{K}{\xi}(\beta[2(p+1)+q])^{\frac{3}{\xi}-1}\Gamma\left(1-\frac{3}{\xi}\right) \quad (14)$$

$$\mu_4 = \frac{K}{\xi}(\beta[2(p+1)+q])^{\frac{4}{\xi}-1}\Gamma\left(1-\frac{4}{\xi}\right) \quad (15)$$

While the variance, skewness, and kurtosis are given respectively:

$$var(x) = \mu_2 - \mu_1^2 = \frac{K}{\xi}(\beta[2(p+1)+q])^{\frac{2}{\xi}-1}\Gamma\left(1-\frac{2}{\xi}\right) - \left(\frac{K}{\xi}(\beta[2(p+1)+q])^{\frac{1}{\xi}-1}\Gamma\left(1-\frac{1}{\xi}\right)\right) \quad (16)$$

$$S = \frac{\mu_3}{(\mu_2)^{\frac{3}{2}}} = \frac{\frac{K}{\xi}(\beta[2(p+1)+q])^{\frac{3}{\xi}-1}\Gamma\left(1-\frac{3}{\xi}\right)}{\left(\frac{K}{\xi}(\beta[2(p+1)+q])^{\frac{2}{\xi}-1}\Gamma\left(1-\frac{2}{\xi}\right)\right)^{\frac{3}{2}}} \quad (17)$$

$$K = \frac{\mu_4}{\mu_2^2} - 3 = \frac{\frac{K}{\xi}(\beta[2(p+1)+q])^{\frac{4}{\xi}-1}\Gamma\left(1-\frac{4}{\xi}\right)}{\left(\frac{K}{\xi}(\beta[2(p+1)+q])^{\frac{2}{\xi}-1}\Gamma\left(1-\frac{2}{\xi}\right)\right)^{2}} - 3 \quad (18)$$

Table 1 shows some values of 1st-4th moment variance, skewness, and kurtosis for OERFR distribution with four sets of parameters.

Table 1. shows some values of 1st-4th moment, variance, skewness, and kurtosis

δ	θ	β	ξ	μ_1	μ_2	μ_3	μ_4	$var(x)$	S	K
1.5	1.2	0.8	1.3	2.133277	4.926708	12.190852	32.049877	0.37583576	0.33545796	2.956465
2.0	1.5	1.0	2.0	2.699500	7.549096	21.816324	65.013273	0.26179344	0.18002620	2.940158
1.0	2.0	1.5	1.5	1.117286	1.277831	1.493741	1.782278	0.02950266	0.02197597	2.850900
0.8	0.9	2.0	2.5	1.074452	1.237086	1.518670	1.979030	0.08263957	0.50076431	3.329302

Table 1 reveals that the distribution exhibits a high degree of adaptability to changing its statistical properties depending on the given parameters. Some groups show a large positive

skewness, reflecting a tail extended to the right, while others exhibit high kurtosis, indicating a concentration of data around the mean with a higher probability of outliers. The variance varies significantly between groups, confirming the distribution's flexibility in representing both low- and high-dispersion data. These results demonstrate that the OERFR is capable of covering a wide range of statistical behaviors depending on the data context.

The moment generating function (MGF) of the OERFR distribution has a form:

$$MGF(y) = \sum_{n=0}^{\infty} \frac{y^n}{n!}\left[\frac{K}{\xi}(\beta[2(p+1)+q])^{\frac{m}{\xi}-1}\Gamma\left(1-\frac{m}{\xi}\right)\right] \quad (19)$$

The Characteristic function of OERFR is derived by employing moments in Eq. (11) and exponential expansion, yielding the form:

$$C_x(y)_{OERFR} = Q_x(t) = \sum_{v=0}^{\infty} \frac{(it)^v}{v!}\left[\frac{K}{\xi}(\beta[2(p+1)+q])^{\frac{m}{\xi}-1}\Gamma\left(1-\frac{1}{\xi}\right)\right] \quad (20)$$

3.3 Incomplete moment

For any random variable X, the moment of order m for OERFR distribution given with Eq. (10) in form [16]:

$$M_m(x) = K\int_0^y x^m x^{-(\xi+1)} e^{-\beta[2(p+1)+q]x^{-\xi}}\,dx$$

$$M_m(x) = K\int_0^y x^{m-(\xi+1)} e^{-\beta[2(p+1)+q]x^{-\xi}}\,dx$$

$$M_m(x) = \frac{K}{\xi}(\beta[2(p+1)+q])^{\frac{m}{\xi}-1}\Gamma\left(1-\frac{m}{\xi},\frac{(\beta[2(p+1)+q])}{y^{\xi}}\right) \quad (21)$$

3.4 Probability Weighted Moments

To calculate the probability weighted moments of OERFR by applying the equation [17]:

$$\tau_{m,t} = E\left(x^m F_{EF}^t(x)\right) = \int_{-\infty}^{\infty} x^m f_{EF}(x) F_{EF}^t(x)\,dx$$

$$\tau_{m,t} = KR\int_0^{\infty} x^m x^{-(\xi+1)} e^{-\beta[2(p+1)+q]x^{-\xi}} e^{-\beta(z+w)x^{-\xi}}\,dx$$

$$\tau_{m,t} = KR\int_0^{\infty} x^{m-(\xi+1)} e^{-\beta[2(p+1)+q+z+w]x^{-\xi}}\,dx$$

$$\tau_{m,t} = \frac{KR}{\xi}(\beta[2(p+1)+q+z+w])^{\frac{m}{\xi}-1}\Gamma\left(1-\frac{1}{\xi}\right) \quad (22)$$

3.5 Quantile function

For every cumulative distribution F(x), the quantile function of order p is defined by the formula [18]:

$Q(q) = \inf\{x \in \mathbb{R}: F(x) \geq q\}$

where q ∈ (0,1)

Or the quantile function is the inverse of CDF, to find the Q(q) for OERFR distribution can be founded as follows:

$$\left(1 - e^{-\delta\left[\frac{e^{-\beta x^{-\xi}}}{1-e^{-\beta x^{-\xi}}}\right]^2}\right)^{\theta} = q$$

$$1 - e^{-\delta\left[\frac{e^{-\beta x^{-\xi}}}{1-e^{-\beta x^{-\xi}}}\right]^2} = q^{\frac{1}{\theta}}$$

$$e^{-\delta\left[\frac{e^{-\beta x^{-\xi}}}{1-e^{-\beta x^{-\xi}}}\right]^2} = 1 - q^{\frac{1}{\theta}}$$

$$-\delta\left[\frac{e^{-\beta x^{-\xi}}}{1-e^{-\beta x^{-\xi}}}\right]^2 = \ln\left(1-q^{\frac{1}{\theta}}\right)$$

$$\left[\frac{e^{-\beta x^{-\xi}}}{1-e^{-\beta x^{-\xi}}}\right]^2 = -\frac{\ln\left(1-q^{\frac{1}{\theta}}\right)}{\delta}$$

Put $T = -\frac{\ln\left(1-q^{\frac{1}{\theta}}\right)}{\delta}$

$$\frac{e^{-\beta x^{-\xi}}}{1-e^{-\beta x^{-\xi}}} = \sqrt{T}$$

$$e^{-\beta x^{-\xi}} = (1-e^{-\beta x^{-\xi}})\sqrt{T}$$

$$e^{-\beta x^{-\xi}} = \sqrt{T} - \sqrt{T}e^{-\beta x^{-\xi}}$$

$$e^{-\beta x^{-\xi}} + \sqrt{T}e^{-\beta x^{-\xi}} = \sqrt{T}$$
$$e^{-\beta x^{-\xi}}\left(1+\sqrt{T}\right) = \sqrt{T}$$
$$e^{-\beta x^{-\xi}} = \frac{\sqrt{T}}{\left(1+\sqrt{T}\right)}$$
$$-\beta x^{-\xi} = \ln\left(\frac{\sqrt{T}}{\left(1+\sqrt{T}\right)}\right)$$
$$x^{-\xi} = -\frac{1}{\beta}\ln\left(\frac{\sqrt{T}}{\left(1+\sqrt{T}\right)}\right)$$
$$Q(q) = Q\left(\left\{-\beta\left[\ln\left(\frac{\sqrt{T}}{\left(1+\sqrt{T}\right)}\right)\right]^{-1}\right\}^{\frac{1}{\xi}}\right)$$

Table 2 shows some values of quantile functions for OERFR distribution with different value of parameters.

$$\frac{1}{x^{\xi}} = -\frac{1}{\beta}\ln\left(\frac{\sqrt{T}}{\left(1+\sqrt{T}\right)}\right)$$
$$x^{\xi} = -\beta\left[\ln\left(\frac{\sqrt{T}}{\left(1+\sqrt{T}\right)}\right)\right]^{-1}$$
$$x = \left\{-\beta\left[\ln\left(\frac{\sqrt{T}}{\left(1+\sqrt{T}\right)}\right)\right]^{-1}\right\}^{\frac{1}{\xi}}$$

Then the final form for moment function is:

(23)

Table 2. Quintile function values for different intervals for δ, θ, β, and ξ

q	$(\delta,\theta,\beta,\xi)$				
	(0.8,0.9,1.1,1.7)	(0.9,0.6,1.4,2.1)	(0.6,1,1.5,1.6)	(0.7,0.8,1.8,1.7)	(1.1,0.9,1.7,2)
0.1	0.8937755	1.005157	1.324868	1.418534	1.367061
0.2	1.0245476	1.147561	1.528157	1.644803	1.527365
0.3	1.1242492	1.257994	1.683255	1.819339	1.647274
0.4	1.2117037	1.355201	1.819557	1.973321	1.751067
0.5	1.2945021	1.446923	1.949019	2.119563	1.848304
0.6	1.3777664	1.538307	2.079633	2.266726	1.945098
0.7	1.4667704	1.634712	2.219824	2.424038	2.047645
0.8	1.5702101	1.744744	2.383692	2.606596	2.165702
0.9	1.7115396	1.891100	2.609184	2.855288	2.325241

Table 2 reveals that the distribution allows for accurate estimation of the boundary values, as the quantile values logically increase with increasing probability. The variation between groups reflects the effect of parameters on the distribution's extent; increasing certain parameters leads to higher boundary values, particularly at higher probability levels. This table provides further evidence of the distribution's ability to represent large or skewed data.

4. Estimation

Let $x_1, x_2, \ldots, x_n$ be a random sample from the OERFR dist.. The likelihood function $L(\Theta)$ is [19-20]:

$$L(\Theta) = \prod_{i=1}^{n} g_{OERFR}(x_i;\delta,\theta,\beta,\xi)$$

$$L(\Theta) = \prod_{i=1}^{n} \frac{2\delta\theta\beta\xi x^{-(\xi+1)}e^{-2\beta x^{-\xi}}}{\left[1-e^{-\beta x^{-\xi}}\right]^3} e^{-\delta\left[\frac{e^{-\beta x^{-\xi}}}{1-e^{-\beta x^{-\xi}}}\right]^2}\left(1-e^{-\delta\left[\frac{e^{-\beta x^{-\xi}}}{1-e^{-\beta x^{-\xi}}}\right]^2}\right)^{\theta-1} \quad (24)$$

Now , the log-likelihood function is

$\ell(\Theta) = \ln L(\Theta)$

$$lnL(\Theta,x) = nln(2) + nln(\delta) + nln(\theta) + nln(\beta) + nln(\xi) - (\xi+1)\sum_{i=1}^{n} ln\,(x_i)$$

$$-2\beta\sum_{i=1}^{n}x_i^{-\xi}-3\sum_{i=1}^{n}ln\left(1-e^{-\beta x^{-\xi}}\right)-\delta\sum_{i=1}^{n}\left[\frac{e^{-\beta x_i^{-\xi}}}{1-e^{-\beta x_i^{-\xi}}}\right]^2$$
$$+(\theta-1)\sum_{i=1}^{n}ln\left(1-e^{-\delta\left[\frac{e^{-\beta x^{-\xi}}}{1-e^{-\beta x^{-\xi}}}\right]^2}\right)$$

The Ordinary Least Squares Estimation (LSE) can be founding by using equation [20]:

$$\varphi(\delta,\theta,\beta,\xi)=\sum_{i=1}^{n}\left[F(x_i)-\frac{1}{n+1}\right]^2$$

$$\varphi(\delta,\theta,\beta,\xi)=\sum_{i=1}^{n}\left[\left(1-e^{-\delta\left[\frac{e^{-\beta x_i^{-\xi}}}{1-e^{-\beta x_i^{-\xi}}}\right]^2}\right)^{\theta}-\frac{1}{n+1}\right]^2 \quad (25)$$

The weighted least squares estimators (WLSE) can be obtained by the equation[20]:

$$\omega(u,r,\alpha)=\sum_{i=1}^{n}\frac{(n+1)^2(n+2)}{i(n-i+1)}\left[F(x_i)-\frac{i}{n+1}\right]^2$$

$$\omega(u,r,\alpha)=\sum_{i=1}^{n}\frac{(n+1)^2(n+2)}{i(n-i+1)}\left[\left(1-e^{-\delta\left[\frac{e^{-\beta x_i^{-\xi}}}{1-e^{-\beta x_i^{-\xi}}}\right]^2}\right)^{\theta}-\frac{i}{n+1}\right]^2 \quad (26)$$

The MLE, LSE, and WLSE $(\hat{\delta},\hat{\theta},\hat{\beta},\hat{\xi})$ are found by simultaneously solving the system of non-linear equations $\frac{\partial\ell}{\partial\delta}=0$, $\frac{\partial\ell}{\partial\theta}=0,\frac{\partial\ell}{\partial\beta}=0$ and $\frac{\partial\ell}{\partial\xi}=0$. The methods must be obtained numerically (using the Newton-Raphson technique, for example) because this system connot be solved analytically.

5. Simulation

The performance of The MLE, LSE, WLSE, Cramer-von Miss (CVM), Anderson-Darling (AD), Maximum Product of Spacings (MPS), Method of Percentile (MP), and Quantile Least Squares (QLS) for the OERFR dist. is evaluated through a Monte Carlo simulation study. The sample in this study are $n = 20, 50, 125$ and 250 to 1000 samples, if abilities are assessed using root mean squared errors (RMSEs) bias measures, and showing in tables 3 [21-22-23].

Table 3: Monte Carlo simulation of OERFR distribution where $\delta = 2.3, \theta = 1.4, \beta = 1.7, \xi = 1.2$

Est.	Est. Par.	$N = 20$							
		MLE	**LSE**	**WLSE**	**CVM**	**AD**	**MPS**	**MP**	**QLS**
Mean	$\hat{\boldsymbol{\delta}}$	4.833445	3.737989	3.675947	3.981592	3.400974	3.972952	2.3517890	5.755513
	$\hat{\boldsymbol{\theta}}$	11.60027	5.132174	6.472154	5.144577	5.98921	8.426768	1.4556969	7.614125
	$\hat{\boldsymbol{\beta}}$	1.6560775	1.6139363	1.5735788	1.6460174	1.5698344	1.4566295	1.6993984	1.8671354
	$\hat{\boldsymbol{\xi}}$	2.1334913	1.3684884	1.3600703	1.5469621	1.4906712	1.5036589	1.2450513	1.5242715

RMSE	$\hat{\delta}$	15.2302	7.977627	7.815627	8.055419	8.216315	13.435857	0.2471499	13.282885
	$\hat{\theta}$	37.33881	11.788321	16.602797	10.022127	16.90833	24.417403	0.1652597	18.619213
	$\hat{\beta}$	1.3013906	0.8313138	0.9180984	0.8584076	0.914062	1.3402702	0.0714269	1.3884489
	$\hat{\xi}$	1.7088213	0.7749586	0.7576939	0.9690611	0.9185617	1.0592434	0.3306261	1.0317880
Bias	$\hat{\delta}$	2.533445	1.437989	1.375947	1.681592	1.100974	1.672952	0.051789	3.455513
	$\hat{\theta}$	10.20027	3.732174	5.072154	3.744577	4.58921	7.026768	0.0556969	6.214125
	$\hat{\beta}$	0.0439224	0.0860636	0.1264212	0.0539825	0.1301656	0.2433705	0.0006015	0.1671354
	$\hat{\xi}$	0.9334913	0.1684884	0.1600703	0.3469621	0.2906712	0.3036589	0.0450513	0.3242715
		$N = 50$							
Mean	$\hat{\delta}$	2.8394226	3.2194268	2.8099091	3.393528	3.1342903	2.4948232	2.3816184	3.2697947
	$\hat{\theta}$	3.738524	3.928556	3.486572	3.943765	3.543196	5.510102	1.4376337	4.064066
	$\hat{\beta}$	1.5935410	1.6416446	1.5689337	1.6772887	1.6195650	1.4176696	1.7015833	1.6592795
	$\hat{\xi}$	1.7506997	1.3787087	1.3940964	1.4653611	1.3943527	1.3853699	1.2056607	1.4772828
RMSE	$\hat{\delta}$	7.5202923	5.6407848	4.6981324	5.930108	5.7422084	5.0002457	0.1744791	5.6834625
	$\hat{\theta}$	11.408492	8.795382	5.915551	7.333176	8.361291	28.507160	0.1112258	9.109321
	$\hat{\beta}$	0.9663639	0.7271653	0.6419937	0.6765421	0.7016574	0.7886702	0.0470790	0.7598441
	$\hat{\xi}$	1.1085767	0.7473766	0.7634836	0.8341377	0.7056878	0.7954154	0.1930824	0.8629042
Bias	$\hat{\delta}$	0.5394226	0.9194268	0.5099091	1.093528	0.8342903	0.1948232	0.0816184	0.9697947
	$\hat{\theta}$	2.338524	2.528556	2.086572	2.543765	2.143196	4.110102	0.0376337	2.664066
	$\hat{\beta}$	0.1064590	0.0583553	0.1310663	0.0227112	0.0804349	0.2823304	0.0015833	0.0407204
	$\hat{\xi}$	0.5506997	0.1787087	0.1940964	0.2653611	0.1943527	0.1853699	0.0056607	0.2772828
		$N = 125$							
Mean	$\hat{\delta}$	2.3416267	2.5725365	2.8014288	2.9959327	2.7147161	2.0466843	2.3895320	3.345572
	$\hat{\theta}$	1.9162949	2.611632	2.254424	2.653865	2.3284572	2.219472	1.4395260	2.677783
	$\hat{\beta}$	1.6315113	1.6092889	1.6628397	1.6766432	1.6272507	1.4450870	1.7044581	1.7206041
	$\hat{\xi}$	1.4814791	1.3082119	1.2849683	1.3285388	1.2784218	1.2243674	1.1862283	1.3946636
RMSE	$\hat{\delta}$	1.9493888	2.7710649	3.9659672	3.5098185	3.4653976	1.6682599	0.1277838	5.453857
	$\hat{\theta}$	1.9891252	3.775128	2.541462	3.297303	2.7829051	1.924634	0.0796607	3.802385
	$\hat{\beta}$	0.4878503	0.4910154	0.5316674	0.5099308	0.5047302	0.5322867	0.0279073	0.6672080
	$\hat{\xi}$	0.7042718	0.5685499	0.5152473	0.6422611	0.5145546	0.4448849	0.1186774	0.7470557
Bias	$\hat{\delta}$	0.0416267	0.2725365	0.5014288	0.6959327	0.4147161	0.2533157	0.0895320	1.045572
	$\hat{\theta}$	0.5162949	1.211632	0.854424	1.253865	0.9284572	0.819472	0.0395260	1.277783
	$\hat{\beta}$	0.0684886	0.0907110	0.0371602	0.0233568	0.0727492	0.2549130	0.0044581	0.0206041
	$\hat{\xi}$	0.2814791	0.1082119	0.0849683	0.1285388	0.0784218	0.0243674	0.0137716	0.1946636
		$N = 250$							
Mean	$\hat{\delta}$	2.3276483	2.4870348	2.2378246	2.3861336	2.2966594	1.9797549	2.3739998	2.7495575
	$\hat{\theta}$	1.6143962	1.9457474	1.7156453	1.8983507	1.7420861	1.868681	1.434813	1.9982008
	$\hat{\beta}$	1.6481935	1.6580886	1.6496291	1.6546363	1.6412603	1.4936601	1.7064610	1.6994598
	$\hat{\xi}$	1.3293598	1.3157239	1.2860237	1.3391389	1.2611584	1.1929029	1.1935657	1.3600213
RMSE	$\hat{\delta}$	1.4877755	2.2767749	1.1168146	2.0547698	1.2957399	1.2016135	0.1053949	3.6429854
	$\hat{\theta}$	1.1290940	1.8368786	1.2121948	1.7111038	1.1896347	1.153142	0.0636184	2.0346098
	$\hat{\beta}$	0.3852565	0.4138902	0.3077935	0.3863027	0.3060834	0.4079970	0.0200013	0.4849630
	$\hat{\xi}$	0.4259332	0.5059569	0.4110650	0.5332621	0.3646219	0.2803577	0.0890675	0.5990113
Bias	$\hat{\delta}$	0.0276483	0.1870348	0.0621754	0.0861336	0.0033405	0.3202451	0.0739998	0.4495575
	$\hat{\theta}$	0.2143962	0.5457474	0.3156453	0.4983507	0.3420861	0.468681	0.034813	0.5982008
	$\hat{\beta}$	0.0518064	0.0419113	0.0503708	0.0453636	0.0587396	0.2063399	0.0064610	0.0005401
	$\hat{\xi}$	0.1293598	0.1157239	0.0860237	0.1391389	0.0611584	0.0070970	0.0064342	0.1600213

Figures 4 to 12 illustrate the plotting of the pdf function for the distribution in terms of the assumed and estimated parameters for the eight methods, and show their effect with different sample sizes for each method.

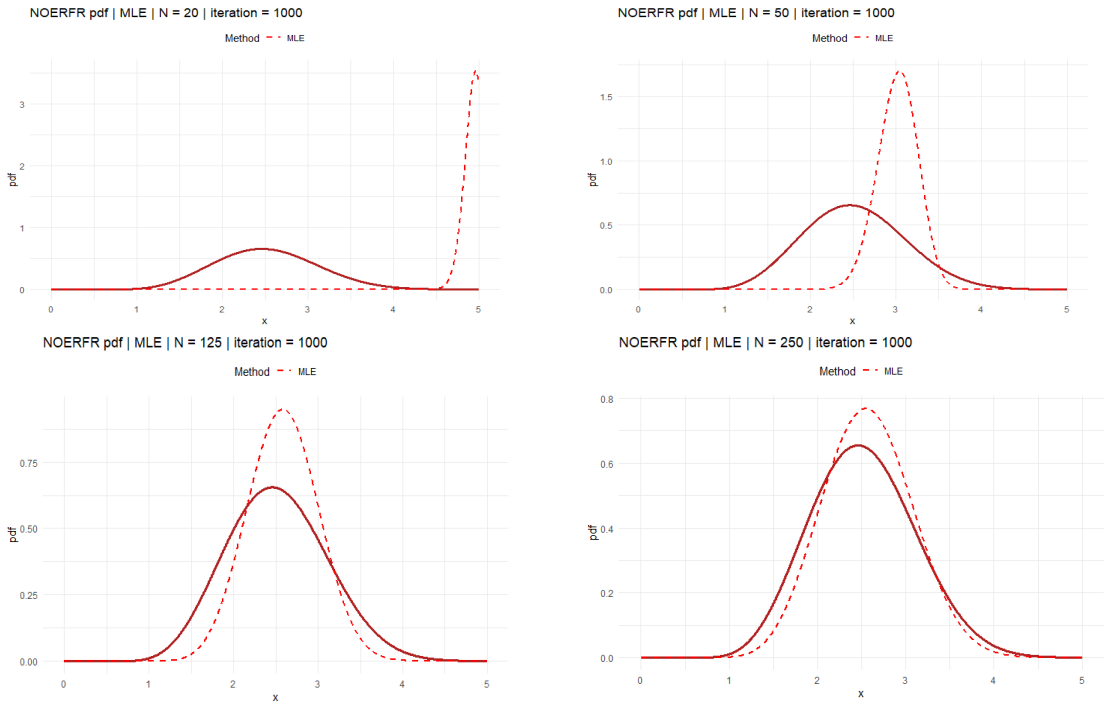

Figure 4. plot survival function pdf function for the distribution in terms of the assumed and estimated parameters for MLE method

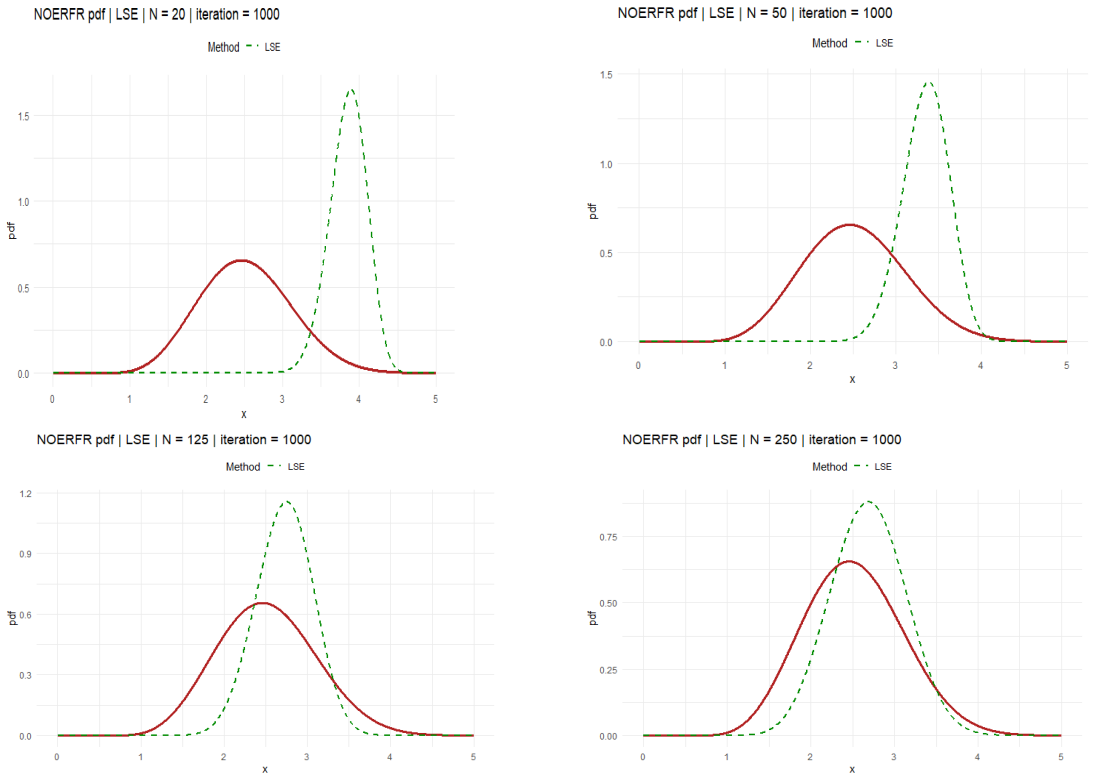

Figure 5. plot survival function pdf function for the distribution in terms of the assumed and estimated parameters for LSE method

Corresponding Author: rwamedh@tu.edu.iq
https://doi.org/10.62933/rqcrpb69

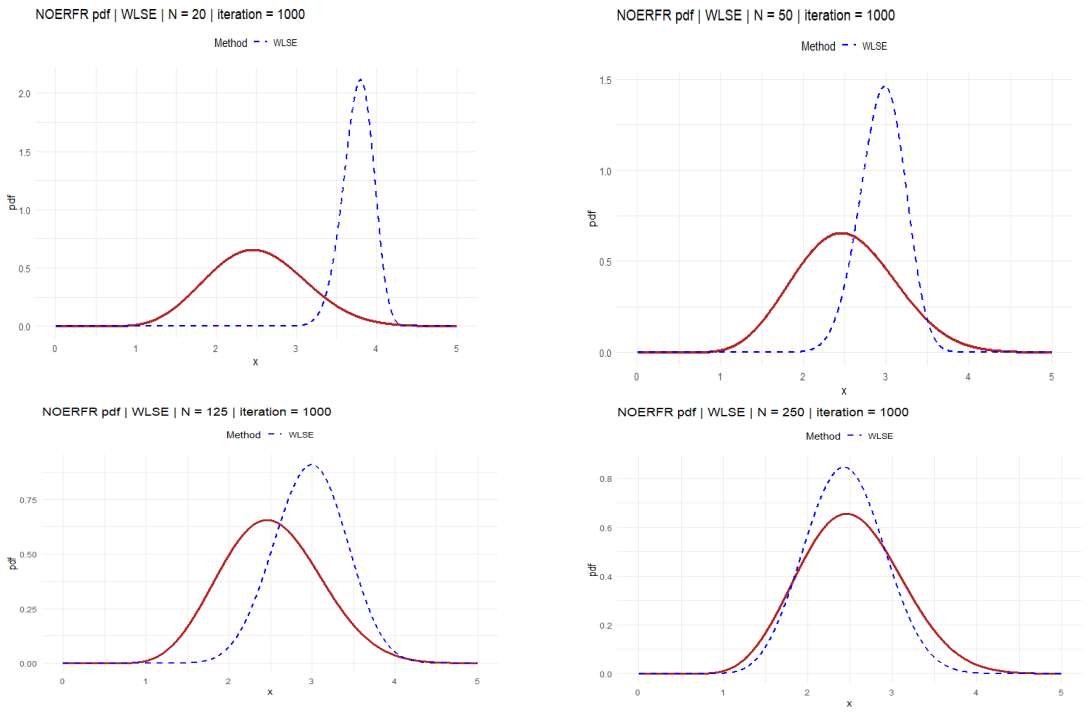

Figure 6. plot survival function pdf function for the distribution in terms of the assumed and estimated parameters for WLSE method

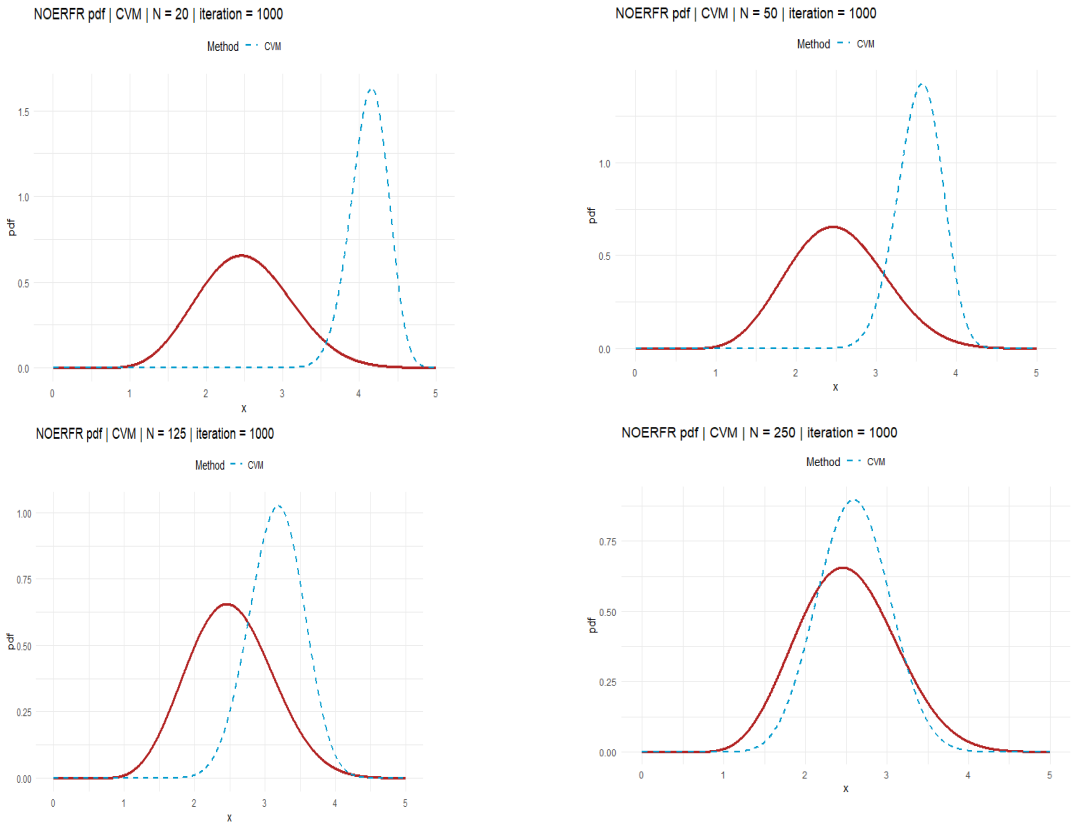

Figure 7. plot survival function pdf function for the distribution in terms of the assumed and estimated parameters for CVM method

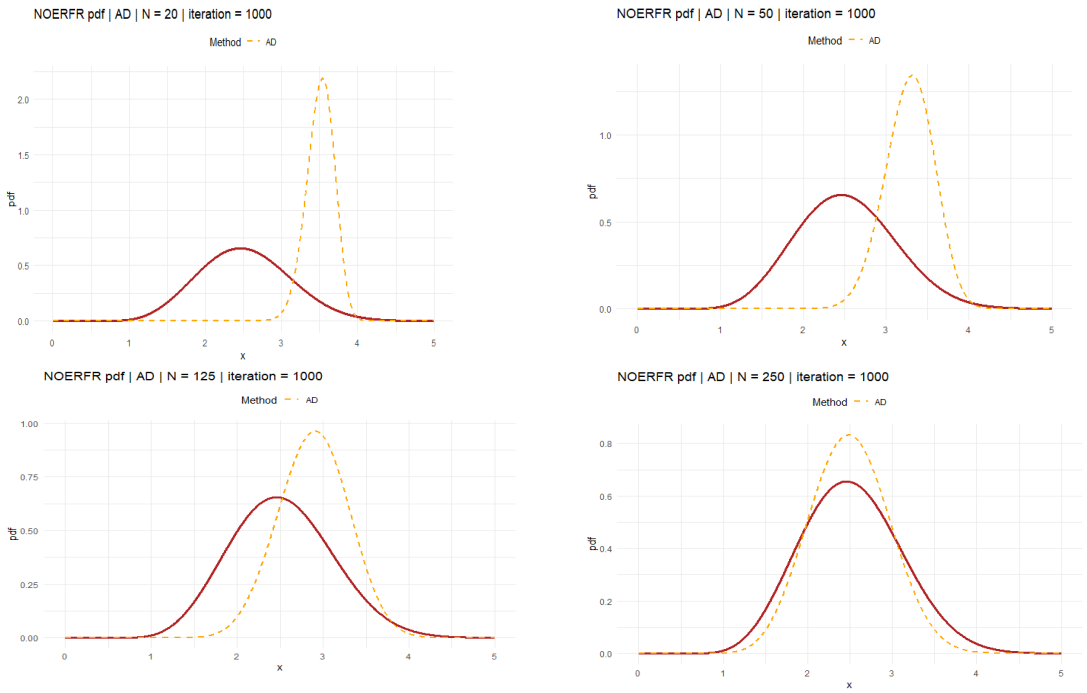

Figure 8. plot survival function pdf function for the distribution in terms of the assumed and estimated parameters for AD method

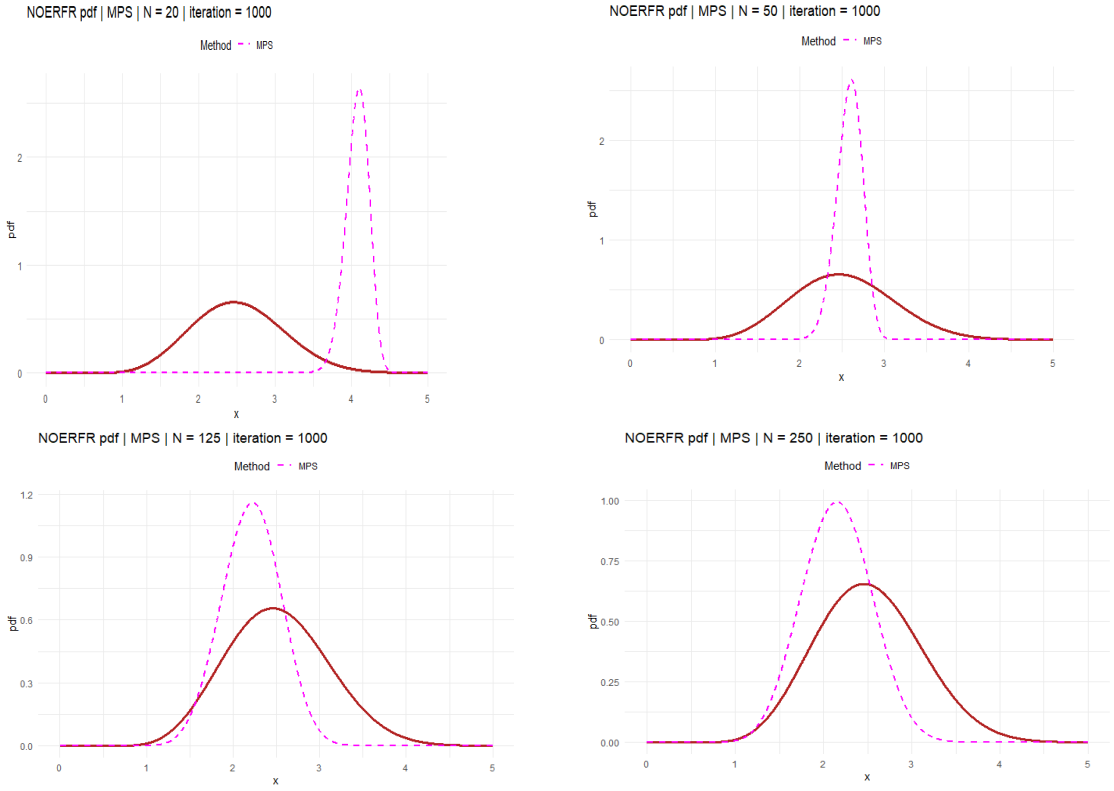

Figure 9. plot survival function pdf function for the distribution in terms of the assumed and estimated parameters for MPS method

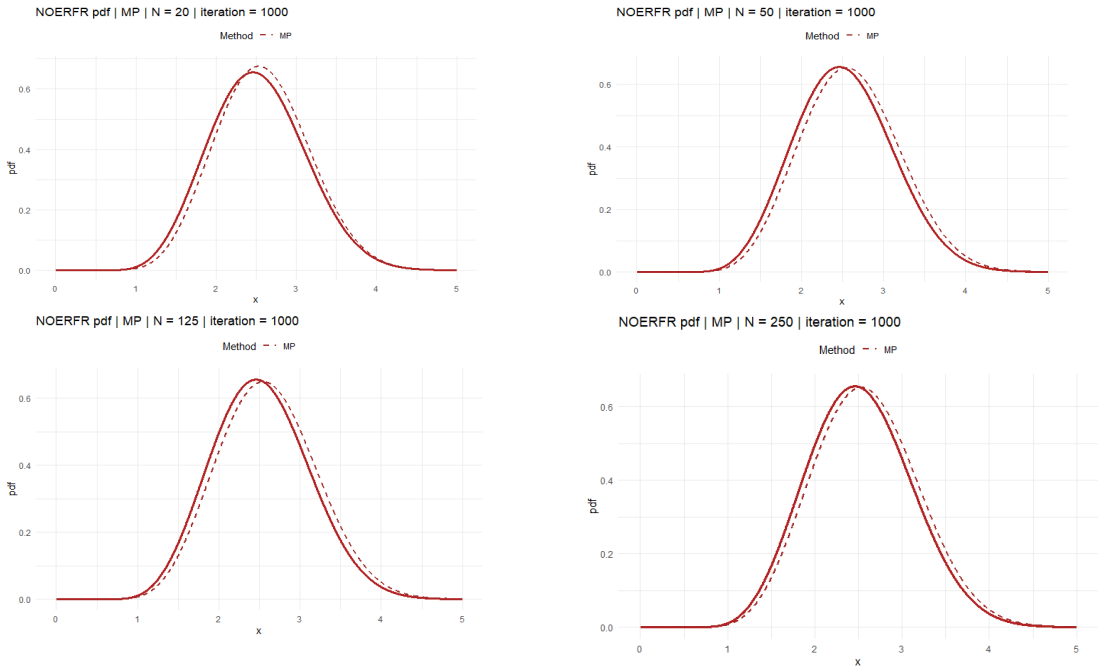

Figure 10. plot survival function pdf function for the distribution in terms of the assumed and estimated parameters for MP method

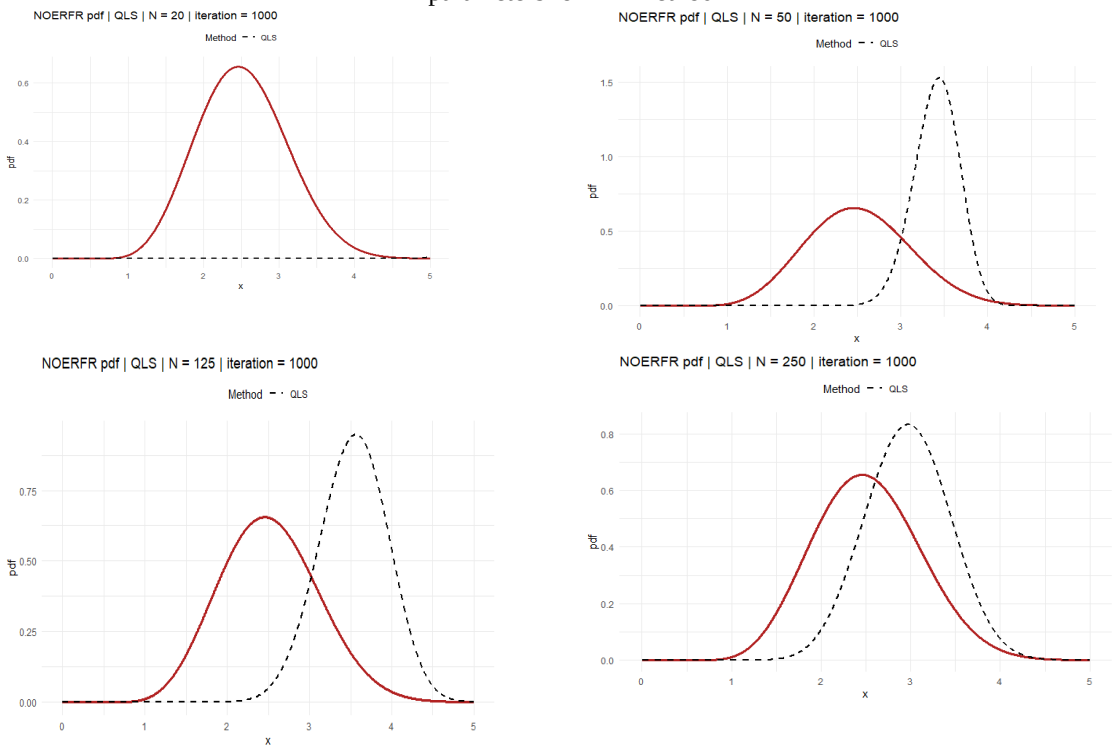

Figure 11. plot survival function pdf function for the distribution in terms of the assumed and estimated parameters for QLS method

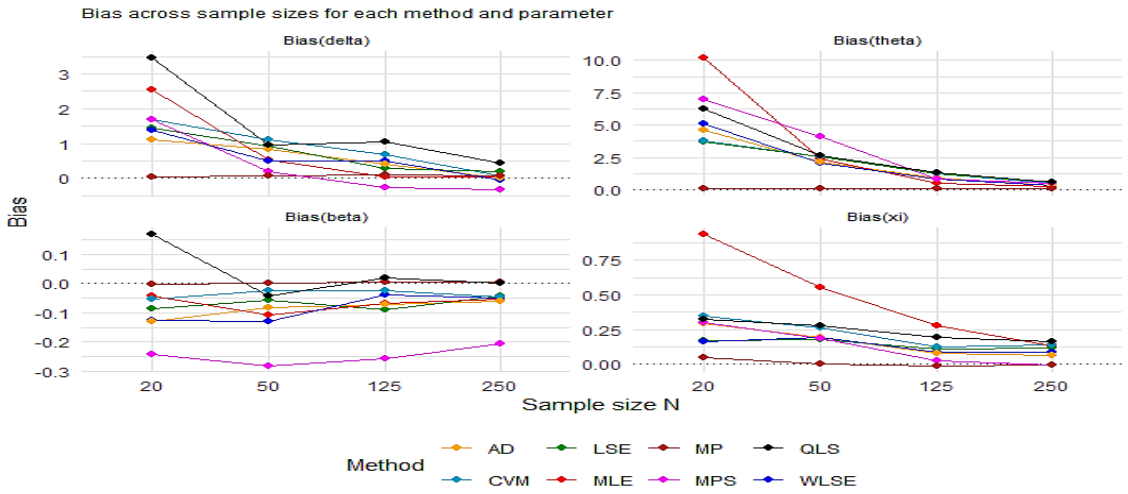

Figure 12. Bias values for the methods and for the four sample sizes

Table 3 presents simulation results for eight estimation methods across a range of sample sizes. The table displays the mean, standard deviation (RMSE), and bias values for each method. It shows that some methods perform better than others for specific samples, and that the quality of the estimate improves as the sample size increases. Methods such as QLS and MP exhibit low RMSE levels and near-zero bias in several cases, while other methods were less stable. These results provide a clear picture of the reliability of each method in estimating the distribution parameters and highlight the superiority of some methods in particular contexts.

Figures 4–11 present a visual comparison between the assumed density function of the distribution and the density function estimated using each of the eight methods. The figures illustrate how closely the estimate approximates the original shape for samples of different sizes. In some methods, such as MLE and WLSE, the estimated curves appear very close to the true function, especially for large samples. Other methods, however, deviate significantly at small sample sizes, indicating their sensitivity to limited samples. This section illustrates how the quality of estimation gradually improves and how these graphs can be used as a practical tool to assess the performance of each method.

Figure 12 shows that bias gradually decreases with increasing sample size. Some methods, such as QLS and MP, exhibit relatively low bias across all sizes, while others show high bias, particularly at small sample sizes. This figure provides a clear visual assessment of the reliability of the methods and highlights the differences in their performance.

5. Real Data Application

To further prove the effectiveness and versatility of the proposed OERFR distribution. Eight measures the Anderson-Darling (A), the Cramér-von Mises statistic (W), the Kolmogorov-Smirnov statistic (KS), the information criteria HQIC, BIC, AIC, and CAIC [24,25-26], and p-value associated with KS test are used in this comparison. These goodness of fit metrics are often employed.

And to demonstrate the structural superiority of the proposed OERFR, we conduct an empirical assessment on two distinct real-world datasets. This practical application aims to showcase the model's enhanced adaptability and its capacity to provide a demonstrably superior goodness-oit compared to several well-established rival distributions.

A real dataset of the time-to-failure (in thousands of hours) of 40 turbocharger units used in diesel engines was studied. The data, originally introduced by Murthy et al. (2004) and revisited in reliability studies by various authors [27-28-29].

The OERFR district with the lowest AIC, AICC, and BIC values in relation to the equivalent values for non-overlapping districts is displayed in Tables 4. and 5. Furthermore, the OERFR distribution is the best match for

the first data set, according to the goodness-of-fit statistics A, W, KS tests, and p-value. However, table 6 displays the MLE-estimated parameters for comparison distances.

Table 4. results of the criteria for the distributions

Data	Dist.	-L	AIC	CAIC	BIC	HQIC
Data set 1	**OERFR**	81.65314	171.3063	172.4491	178.0618	173.7489
	BeFR	87.23679	182.4736	183.6164	189.2291	184.9162
	KuFR	86.88725	181.7745	182.9174	188.53	184.2171
	EGFR	86.8627	181.7254	182.8683	188.4809	184.168
	WeFR	82.84992	173.6998	174.8427	180.4554	176.1424
	GoFR	86.40257	180.8051	181.948	187.5607	183.2477
	FR	101.5918	207.1836	207.5079	210.5613	208.4049

Table 5. results of the criteria for the distributions

Data	Dist.	W	A	K-S	p-value
Data set 1	**NOERFR**	0.07163563	0.5448256	0.1129271	0.7160864
	BeFR	0.2016845	1.345759	0.1553162	0.2894776
	KuFR	0.1916131	1.282165	0.1278271	0.5304583
	EGFR	0.1946524	1.304336	0.1485352	0.3406598
	WeFR	0.08777913	0.6446357	0.1138428	0.7095174
	GoFR	0.1829746	1.235169	0.141056	0.4037099
	FR	0.6068011	3.479705	0.2437845	0.01722618

Tables 4 and 5 present the results of a comparison between OERFR and several competing distributions using well-known metrics such as AIC, BIC, CAIC, HQIC, and quality of fit measures KS, A, and W. The results show that the OERFR distribution outperforms the other distributions in almost all metrics, indicating its high fit to real data. The low AIC and BIC values suggest that the model achieves a balance between accuracy and simplicity. The KS and p-value results show a good match between the distribution and the data.

Table 6. MLE the distributions

Data	Dist.	W	A	K-S	p-value
Data set 1	**NOERFR**	0.003417806	0.518330135	2.509501901	2.555174549
	BeFR	0.3067965	48.5091480	29.5676932	1.1467567
	KuFR	4.7878179	200.3656490	8.0418712	0.5715006
	EGFR	66.1840895	0.3246714	30.3776149	1.1163471
	WeFR	30.7193539	0.4917666	3.9631375	0.1009654
	GoFR	92.6195384	0.3832491	38.8101544	0.9736837
	FR	---	---	4.671924	1.944636

Table (6) contains the parameter values of the distributions estimated using the MLE method for real data. The table illustrates the magnitude of the difference between the proposed distribution and other estimated distributions, revealing OERFR's ability to provide stable and reasonable parameter values compared to other models that exhibit significant variability. These results support the adoption of OERFR in practical modeling.

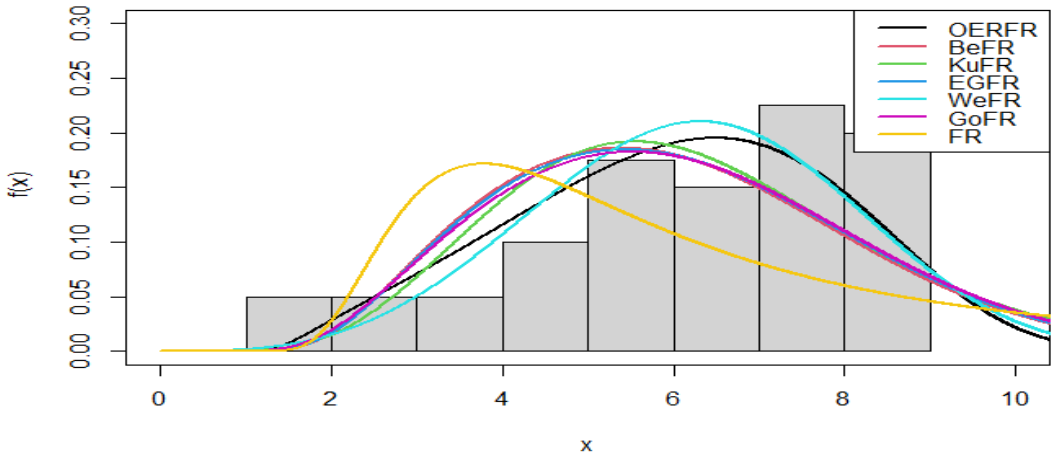

Figure 13. Fitted densities for the Data set

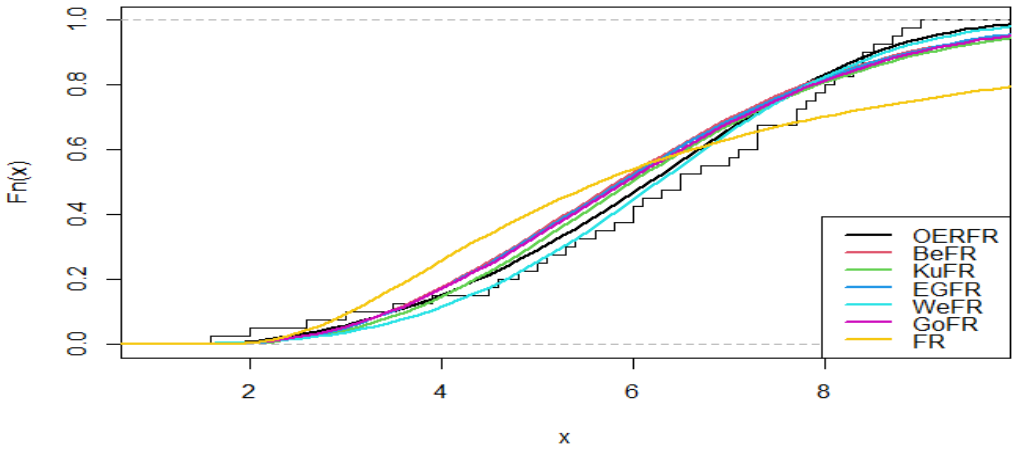

Figure 14. Empirical CDF for the Data set

Figure 13 shows the fit of the probability densities to the data, clearly demonstrating that the OERFR curve is the closest to the data shape compared to competing models. Figure 14 presents the empirical versus theoretical distribution functions, also revealing that OERFR exhibits the best agreement, with its curve closely approximating the empirical line without significant deviation. These results confirm the practical superiority of the proposed model.

Conclusions

Mathematical and applied analysis of the proposed distribution reveals that the OERFR model offers a significant expansion of the families of exotic distributions with high adaptability to complex data. Derivatives show that adding new shape parameters gives the distribution broad control over tail behavior and density slope, allowing for accurate representation of data with extreme values. Sequential expansions have proven highly effective in simplifying theoretical calculations and estimating moments without requiring complex closed solutions. Simulation experiments have also demonstrated that the performance of estimation methods varies with sample size and that the model maintains statistical stability for most estimation methods. Practical application to real data has shown the clear superiority of the OERFR distribution over all competing distributions, yielding the smallest values for statistical information measures and the highest degree of agreement with the empirical distribution function. These results indicate that the distribution represents a practical and reliable addition to probability modeling and is a preferred choice for analyzing dependency, engineering, and extreme values data, opening the door to deeper studies involving binary

generalizations and linking the model to risk-increasing processes in industrial applications.

Conflicts of interest

Non

References

[1] Alzaatreh, A., Lee, C., & Famoye, F. (2013).A new method for generating families of continuous distributions using the T-X family. *Journal of Statistical Distributions and Applications*.

[2] A. S. Hassan, A. I. Al-Omari, R. R. Hassan and G. A. Alomani , "The odd inverted Topp Leone–H family of distributions: Estimation and applications," *Journal of Radiation Research and Applied Sciences,* pp. 365-379, 3 15 2022.

[3] J. T. Eghwerido, F. I. Agu and O. J. Ibidoja, "The shifted exponential-G family of distributions: Properties and applications," *Journal of Statistics and Management Systems,* pp. 43-75, 1 25 2022.

[4] Y. Wang, Z. Feng and A. Zahra, "A new logarithmic family of distributions: Properties and applications," *CMC-Comput. Mater. Contin,* p. 919–929, 66 2021.

[5] Z. Shah, D. M. Khan, Z. Khan, N. Faiz, S. Hussain, A. Anwar, T. Ahmad and K.-I. Kim, "A new generalized logarithmic–X family of distributions with biomedical data analysis," *Applied Sciences,* p. 3668, 6 13 2023.

[6] S. Hussain, M. U. Hassan, M. S. Rashid and R. Ahmed, "Families of Extended Exponentiated Generalized Distributions and Applications of Medical Data Using Burr III Extended Exponentiated Weibull Distribution," *Mathematics,* p. 3090, 14 11 2023.

[7] N. A. Noori, A. A. Khalaf and M. A. Khaleel, "A New Generalized Family of Odd Lomax-G Distributions Properties and Applications," *Advances in the Theory of Nonlinear Analysis and Its Application,* pp. 1-16, 4 7 2023.

[8] A. I. Ishaq, U. Panitanarak, A. A. Alfred , A. A. Suleiman and H. Daud, "The Generalized Odd Maxwell-Kumaraswamy Distribution: Its Properties and Applications," *Contemporary Mathematics,* pp. 711-742, 2024.

[9] G. A. Mahdi, M. A. Khaleel, A. M. Gemeay, M. Nagy , A. H. Mansi, M. M. Hossain and E. Hussam, "A new hybrid odd exponential-Φ family: Properties and applications," *AIP Advances,* 4 14 2024.

[10] N. Salahuddin, Alamgir, M. Azeem, S. Hussain and M. Ijaz, "A novel flexible TX family for generating new distributions with applications to lifetime data," *Heliyon* , p. e36593, 17 10 2024.

[11] Al-Shomrani, A. A., Arif, O. H., Shawky, A., Hanif, M., & Shahbaz, M. Q. (2016).Topp–Leone family of distributions: Some properties and applications. *Pakistan Journal of Statistics and Operation Research*, *12*(3), 439–451.

[12] Abed, R., Khaleel, M., & Noori, N. (2025). Modified Weibull-Fréchet Distribution Properties with Application. *Iraqi Statisticians journal*, 195-216.

[13] Dias, C. R. B., Alizadeh, M., & Cordeiro, G. M. (2018). The beta Nadarajah–Haghighi distribution. *Hacettepe Journal of Mathematics and Statistics*, *47*(5), 1302–1320

[14] Nadarajah, S., Cordeiro, G. M., & Ortega, E. M. M. (2013).
The gamma-G family of distributions: Mathematical properties and applications. *Communications in Statistics – Theory and Method*s

[15] Noori, N., & Khaleel, M. (2025). The Modified Burr-III Distribution Properties, Estimation, Simulation, with Application on Real Data. *Iraqi Statisticians journal*, *2*(special issue for ICSA2025), 225-246.

[16] Khelliel, A. H., *et al.* (2022). Inverse Weibull family of distributions: Properties and applications. *Journal of Statistical Theory and Applications*, *21*(4), 661–680

[17] Banerjee, P., & Bhunia, S. (2022). Exponential transformed inverse Rayleigh distribution: Statistical properties and different methods of estimation. *Austrian Journal of Statistics*, *51*(4), 60–75.

[18] Noori, N. A., Khaleel, M. A., Alharigy, T. M., Almetwally, E. M., & Elgarhy, M. (2026). The Neutrosophic Gompertz-G Family: Analytical Properties, Simulation Studies, and Applications to Real Data. *Modern Journal of Statistics*, *2*(1), 75-99.

[19] Norouzirad, M., Rao, G. S., & Mazarei, D. (2023). Neutrosophic generalized Rayleigh distribution with application. *Neutrosophic Sets and Systems*, *58*, 248-262.

[20] Jumaa, M. H., Qaddoori, A. S., Khalaf, S. A., Noori, N. A., & Khaleel, M. A. (2025). Mathematical Properties and Simulations of the Neutrosophic Gompertz-Inverse Burr-X Distribution with Application to Under-Five Mortality. *Iraqi Journal for Computer Science and Mathematics*, *6*(3), 23.

[21] Husain, Q. N., Qaddoori, A. S., Noori, N. A., Abdullah, K. N., Suleiman, A. A., & Balogun, O. S. (2025). New Expansion of Chen Distribution According to the Nitrosophic Logic Using the Gompertz Family.

[22] Shah, F., Aslam, M., Khan, Z., Almazah, M. M., & Alduais, F. S. (2022). [Retracted] On Neutrosophic Extension of the Maxwell Model: Properties and Applications. *Journal of Function Spaces*, *2022*(1), 4536260.

[23] Noori, N. A., Khaleel, M. A., Khalaf, S. A., & Dutta, S. (2025). Analytical Modeling of Expansion for Odd Lomax Generalized Exponential Distribution in Framework of Neutrosophic Logic: a Theoretical and Applied on Neutrosophic Data.

[24] Zeghbib, F. Z., & Zeghdoudi, H. (2026). The Neutrosophic New XLindley Distribution: Statistical Properties, Estimation, Simulation, and Application. *Neutrosophic Sets and Systems*, *97*, 205-215.

[25] Saleem, M., Bashir, S., Tayyab, A., Aslam, M., & Rasul, M. (2025). Neutrosophic Gompertz Distribution: Applications in Analyzing Complex

Environmental Datasets. *International Journal of Computational Intelligence Systems*, *18*(1), 1-20.

[26] Noori, N. A., Khaleel, M. A., & Salih, A. M. (2025). Some Expansions to The Weibull Distribution Families with Two Parameters: A Review. *Babylonian Journal of Mathematics*, *2025*, 61-87.

[27] Abd El-latif, A. M., Alqasem, O. A., Okutu, J. K., Tanış, C., Sapkota, L. P., & Noori, N. A. (2025). A flexible extension of the unit upper truncated Weibull distribution: Statistical analysis with applications on geology, engineering, and radiation Data. *Journal of Radiation Research and Applied Sciences*, *18*(2), 101434.

[28] Abdullah, H. H., Khalaf, N. S., & Noori, N. A. (2024). Comparison of non-linear time series models (Beta-t-EGARCH and NARMAX models) with Radial Basis Function Neural Network usingReal Data. *Iraqi Journal For Computer Science and Mathematics*, *5*(3), 38.

[29] Nawaf, A. J., Jumaa, M. H., Noori, N. A., & Khaleel, M. A. (2024, October). Search and Expand Hybrid Odd Lomax Fréchet Distribution Properties, Simulation, with Application. In *UiTM International Conference on Mathematical Sciences* (pp. 193-218). Singapore: Springer Nature Singapore.